PRODUCT COMPOSITION AND KINETICS OF LIGNITE PYROLYSIS

Eric M. Suuberg, William A. Peters, and Jack B. Howard

Department of Chemical Engineering and Energy Laboratory
Massachusetts Institute of Technology
Cambridge, Massachusetts 02139

SUMMARY

The pyrolysis of pulverized Montana lignite by time-resolved measurement of the yields and compositions of products formed under controlled temperature-time histories was studied in a captive sample apparatus. A thin layer of particles held in a folded strip of stainless steel screen was electrically heated under both 1 atm helium and vacuum in a vessel connected to a series of product recovery traps. The temperature of the sample was measured with a thermocouple. Heating rate, peak temperature attained, and residence time at the peak temperature were independently varied in the ranges 100-10^4°C/s, 150-1100°C, and 0-10s. The yields of char and tar were determined gravimetrically and selected char samples were subjected to elemental analysis. The yields of water, carbon monoxide, carbon dioxide, hydrogen, and hydrocarbon gases and light liquids were determined by gas chromatography.

The yields of all the volatile products increase monotonically with temperature and approach asymptotic values at the higher temperatures. At 1000°C/s and 1 atm helium the ultimate yields, in percent by weight of the lignite (as-received), are 16.5 % water (including 6.8 % moisture), 9.5 % carbon dioxide, 9.4 % carbon monoxide, 5.4 % tar, 1.3 % methane, 0.6 % ethylene, 0.5 % hydrogen, and 0.9 % ethane, propylene, propane, benzene, and trace hydrocarbons. The total yield of 44.0 % is close to the ASTM volatile matter plus moisture (43.7 %). Pyrolysis at the higher temperatures volatilizes about 70 % of the sulfur and about 25 % of the nitrogen; the percent by weight of sulfur in the char is less than that in the lignite but the reverse is true for nitrogen.

The individual product yields vary with temperature in a series of steps indicative of the occurrence of five principal phases of devolatilization: moisture evolution at about 100°C; a large initial evolution of carbon dioxide beginning at about 450°C, probably from decarboxylations, and a small amount of tar formation; evolution of chemically formed water and a small amount of carbon dioxide at 500-700°C; rapid evolution of carbon monoxide, carbon dioxide, tar, hydrogen, hydrocarbon gases, and only little water at 700-900°C; high-temperature formation of carbon monoxide and carbon dioxide. The kinetics of the production of each product is modelled with one to three independent parallel first-order reactions. The frequency distribution of all the activation energies derived for the various products by fitting the present composition data agrees well with the Gaussian distribution obtained previously from weight loss data for the same lignite.

INTRODUCTION

Previous research at M.I.T. on coal pyrolysis in inert gas and in hydrogen was based on the measurement of coal weight loss, referred to as volatiles yield(1-5). The work is now being extended to include volatiles composition measurements and elemental analysis of the char for the same ranges of experimental conditions covered in the previous study. To this end, the previous apparatus has been modified to permit the collection and analysis of volatiles. This paper presents the first set of composition data, for lignite pyrolysis, and some initial interpretations of pyrolysis behavior in the light of the products formed.

APPARATUS AND PROCEDURE

The apparatus (Fig. 1) consists of five components: the reactor, designed to contain a coal sample in a gaseous environment of known pressure and composition; the electrical system, used to expose the sample to a controlled time-temperature history; the time-temperature monitoring system; the product collection system; and the product analysis system.

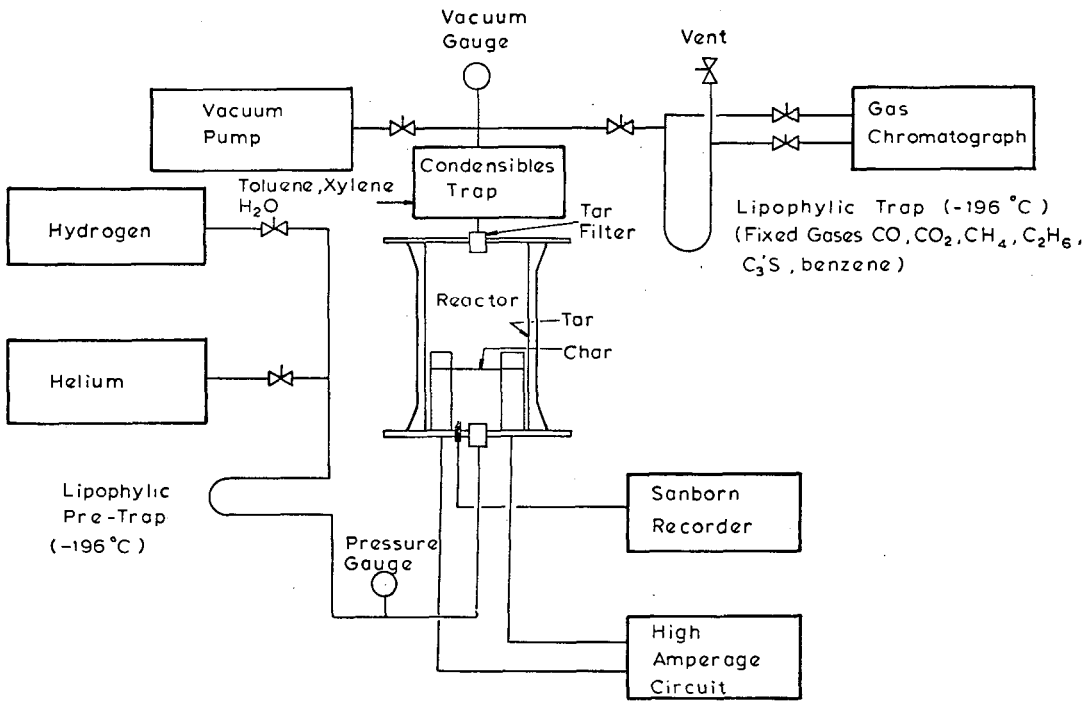

Figure 1. Captive Sample Apparatus and Analysis System.

The reactor, designed for atmospheric-pressure and vacuum pyrolysis work, consists of a 6-inch (15.24 cm) long, 3-inch (7.62 cm) diameter pyrex glass pipe, blind-flanged at both ends by stainless steel plates having electrical feedthroughs and gas inlet and outlet ports. The coal sample is held and heated in the vessel by a folded strip of 325 mesh stainless steel screen positioned between two relatively massive brass electrodes as shown in Fig. 2.

The electrical system consists of two automobile storage batteries connected in series to the reactor electrodes through a timer-controlled relay switch which cuts in either of two variable resistors at a predetermined time. This circuitry permits independent control of heating rate (10^2-10^4°C/s) and final sample holding time and temperature (150-1100°C for up to 30 s). The temperature-time history of coal is recorded by a chromel-alumel thermocouple (24 μm wire diam., 75 μm bead diameter) placed within the sample and connected to a Sanborn fast-response recorder.

Approximately 10-15 mg of powdered coal is spread in a layer one to two particles deep on a preweighed screen which is reweighed and inserted between the brass electrodes. The reactor is evacuated and flushed three to five times with helium and then set at the desired experimental pressure. The sample temperature is raised at a desired rate to a desired holding value which is then maintained until the circuit is broken. Sample cooling by convection and radiation then occurs rapidly since the electrodes, the vessel and its gaseous contents remain cold during the experiment, but not so rapidly as to avoid the occurrence of significant weight loss during cooling.

The yield of char, which remains on the screen, is determined gravimetrically. Products that condense at room temperature (tars and oils, hereafter defined as tars) are collected primarily on foil liners within the reactor and on a paper filter at the exit of the reactor. Any condensation on non-lined reactor surfaces is collected by washing with methylene chloride soaked filter paper. The tar from all three collections is measured gravimetrically.

Products in the vapor phase at room temperature are collected at the conclusion of a run by purging the reactor vapors through two lipophilic traps. The first trap consists of a 3 inch (7.62 cm) long, 1/4 inch (0.635 cm) diameter tube containing 50/80 mesh Porapak Q chromatographic packing. The trap is operated at room temperature, and collects intermediate weight oils such as benzene, toluene, and xylene. The second trap is a 15 inch long, 1/4 inch diameter tube (38.1 cm x 0.625 cm) also packed with Porapak Q but operated at -196°C in a dewar of liquid nitrogen. This trap collects all fixed gases produced by pyrolysis, with the exception of hydrogen which is determined by direct vapor phase sampling with a precision syringe.

Products are recovered for gas chromatographic analysis by warming the first trap to 240°C and the second to 100°C. The intermediate weight oils from the first trap are analyzed on either a 50/80 mesh, 3 % OV-17 or Porapak Q column, 6 ft x 1/8 in (183 cm x 0.318 cm). The fixed gases from the second trap are analyzed on a 12 ft x 1/4 in (366 cm x 0.635 cm) 50/80 mesh Porapak Q column, temperature programmed from -70 to 240°C at a rate of 16°C/min. The hydrogen is analyzed on a 10 ft x 1/8 in (305 cm x 0.318 cm) 80/100 mesh Spherocarb column at 0°C. A Perkin-Elmer Model 3920 B chromatograph with dual thermal conductivity/flame ionization detectors and a Perkin-Elmer Model 1 integrator are used for all the analyses.

Elemental analyses of the raw coal and char samples were performed by Galbraith Laboratories, Inc. of Knoxville, Tennessee.

The weight of the coal and screen was determined to within ±0.01 mg; hence, the uncertainty of the total weight loss measurement is about 0.1 % by weight of the coal. The products quantitated chromatographically (except H_2O) are subject to calibration uncertainties of 1 to 3 % of the mass of the species measured. The water measurements were somewhat more troublesome because of (1) moisture loss from the coal during the short time lapse between weighing the sample and performing the run and (2) moisture gain by the experimental system during assembly under high humidity conditions. The net uncertainty in the measured water yields caused by these opposing effects is about 2 % by weight of the coal. The tar measurement

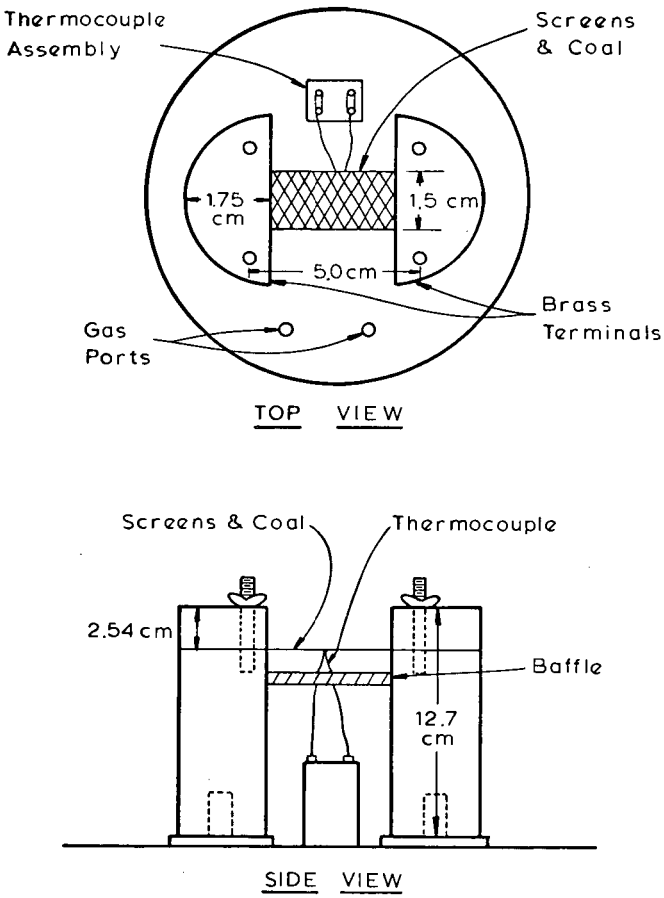

Figure 2. Sample Holding and Heating Assembly.

has its largest uncertainty in the washing procedure. The maximum error for atmospheric pressure runs is about 1 % by weight of the coal. The inherent uncertainty of the thermocouple measurements is about ± 8°C over the present range of temperatures. The ability of the selected thermocouple effectively to track the temperature of the sample at the highest heating rates was confirmed by experiments with thermocouples of different bead diameters.

Some discoloration of the screen used to hold the sample caused concern that the screen may be a source of error, for example through catalysis of primary pyrolysis or secondary cracking reactions. Experimental assessment of the role of the screen included passivation of the surface with a vacuum deposited layer of gold on some screens and copper on others, and variation of the number of layers of untreated screen through which the volatiles had to escape. Both gold and copper are less catalytic to cracking reactions than is stainless steel, and diffusion of these metals in stainless steel is too slow to destroy the integrity of the surface layer in even the longest residence times of this study. None of these cases lead to significant differences in the total yield of volatiles or in the composition of gaseous products included in the present study. Therefore, any error caused by the screen appears to be negligible for present purposes. This result is not surprising in view of the high escape velocity of volatiles from the sample and hence the low residence time of volatiles near hot screens. Nevertheless, untreated stainless steel screens in a similar apparatus are reported(6) to react significantly with hydrogen sulfide. This species is not of present concern.

RESULTS

All the results here reported are for a partially dried (as-received) Montana lignite (Savage Mine, Knife River Coal Co.) in the particle size range 53-88 μm (74 μm average diameter) (Table 1).

Table 1. Characteristics of the Partially Dried Lignite

Proximate Analysis, Wt.%(as-received)		Ultimate Analysis, Wt.%(as-received)		Petrographic Analysis (Wt.%(mineral-matter-free)	
Moisture	6.8	Carbon	59.3	Vitrinites	69.7
V.M.	36.9	Hydrogen+	4.5	Semi-Fusinite	15.2
F.C.	46.4	Nitrogen	0.9	Fusinite	7.9
Ash	9.9	Sulfur	1.1	Micronite	5.2
Total	100.0	Oxygen*+	17.5	Exinite	2.0

* By difference, using measurements of other elements, moisture and ash.
\+ Exclusive of moisture content.

Base Data With the exception of the data points carrying a double symbol (see below), the volatile product compositions shown in Fig. 3 were obtained when different samples of the lignite under 1 atm (101.3 kPa) of helium were heated at approximately 1000°C/s to various peak temperatures indicated on the abscissa. The samples were cooled at roughly 200°C/s beginning immediately when the peak temperature was attained. The total yield of any product or group of products is given on the ordinate as a weight percent of the partially dried lignite.

The lowest curve represents the yield of tar as defined above, which increases with increasing temperature to an asymptotic maximum of about 5.4 % by weight of the lignite at temperatures above 750 to 800°C. The tar appears to have two primary components. One is a heavy, tawny brown liquid-like material which deposits as a film on surfaces. The other consists of dark brown objects which give the impression of being solid pieces of lignite that were presumably broken off of the parent material and carried away with the volatiles. These "particles", some

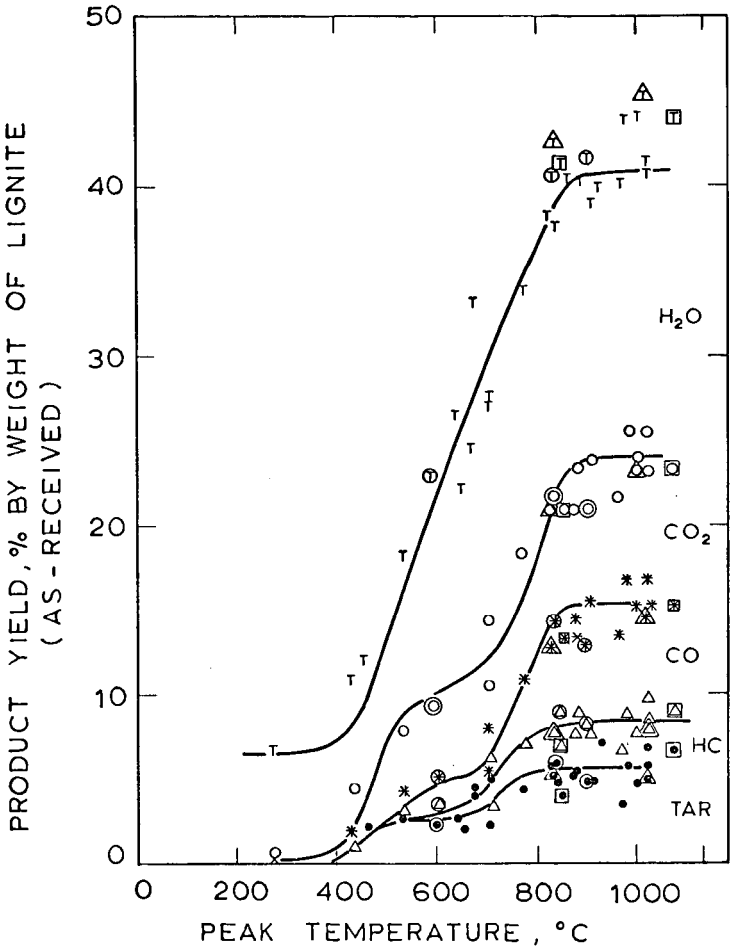

Figure 3. Pyrolysis Product Distributions from Lignite Heated to Different Peak Temperatures. [(●) tar; (Δ) tar and other hydrocarbons (HC); (*) tar, HC, and CO; (o) tar, HC, CO and CO_2; (T) total, i.e., tar, HC, CO, CO_2, and H_2O. Pressure = 1 atm (helium). Heating rate:(single points) 1000°C/s; (points inside O) 7,100 to 10,000°C/s; (points inside Δ) 270 to 470°C/s; (points inside □) 1000°C/s but two-step heating. (curves) First-order model using parameters shown in Table 5].

of which appear to be agglomerates, are for the most part smaller than 10 μm across but sometimes as large as 25 μm. About 75 % of the tar including most of the tawny liquid and a fraction of the particles appears to dissolve in methylene chloride. Extensive analysis of any one tar sample is difficult because of the small yields.

The distance between the tar curve and the next one above it represents hydrogen and all hydrocarbons lighter than tar. The maximum yield of these species occurs at the higher temperatures and is only about 3.3 % by weight of the lignite. The main components are methane (1.3 %), ethylene (0.6%), and hydrogen (0.5 %), with identified ethane, propylene, propane, and benzene and unidentified trace hydrocarbons making up the balance. The effect of temperature on yields of methane, hydrogen and ethylene is shown in Fig. 4. When the peak temperature is increased above 500°C the methane and ethylene yields increase rapidly to small asymptotic values in the range 600 - 700°C. Further increase in temperature beyond 700°C effects a dramatic increase in the yield of both species, and a second asymptote is reached at about 850°C for ethylene and about 900°C for methane. The yield of tar also exhibits a similar two-step behavior but hydrogen production, on the other hand, appears to occur in one step at relatively high temperatures.

The top curve in Fig. 3 represents the total yield of volatiles while, proceeding downward, the first, second and third regions between adjacent curves represent the yields of water, carbon dioxide, and carbon monoxide, respectively. The yields of these principal oxygenated species are shown in more detail in Fig. 5 where all three appear to approach high-temperature asymptotic yields of 16.5 % for water, 8.4 % for carbon dioxide, and 7.1 % for carbon monoxide. The carbon oxides each exhibit also a lower-temperature asymptote.

Although most of the pyrolysis is complete for peak temperatures above about 900 to 1000°C, there is in fact yet a third step in the curves for the carbon oxides which occurs at about 1100°C and therefore does not appear in Fig. 5. Since this temperature is the upper limit of the apparatus, investigation of this third step was accomplished by use of a longer residence time technique. The coal was heated at 1000°C/s to 1000°C and there held for 5 to 10 s rather than being immediately cooled as before. The resulting carbon monoxide yield exhibits a final asymptote of 9.4 % while that of carbon dioxide is 9.5 %. The yields of the other species were not changed by the additional residence time. Thus prolonged heating at 1000°C gave a total volatiles yield of 44.0 % by weight of the lignite which is close to the ASTM volatile matter plus moisture (43.7 %).

Elemental analyses of selected char samples are shown in Fig. 6. Although over 40 % by weight of the lignite is volatilized at the higher temperatures, only 22 % of the carbon is volatilized. Most of the volatile material comes from hydrogen and oxygen, which is consistent with the observed predominance of water among the volatile products. Pyrolysis at the higher temperatures removes about 70 % of the sulfur from the solid material, but the nitrogen is reduced by only about 25 %. Consequently, the sulfur content (percent by weight) in the char is lower than that of the lignite, but the reverse is true for nitrogen. Similar data obtained by Kobayashi et al.(7,8) in an entrained flow reactor show that the fractional evolutions of sulfur and nitrogen are increased to at least 85 % and 65 %, respectively, as the pyrolysis of Montana lignite is extended to 1800°C. The weight of ASTM ash in the char from most of the present experiments is less than that in the raw lignite, which is qualitatively similar to a previous observation(7,8).

Elemental balances were calculated for runs in which both volatile products and char were analyzed. For estimation purposes, tar and trace hydrocarbons (total less then 1 % by weight of the lignite) were assumed to be 90 % carbon and 10 % hydrogen by weight. Typical results for four runs to different peak temperatures are presented in Table 2 along with total mass balances. Whereas the mass balances are excellent and the carbon and hydrogen balances are satisfactory, the oxygen balances are marginal. Since oxygen in char is determined by

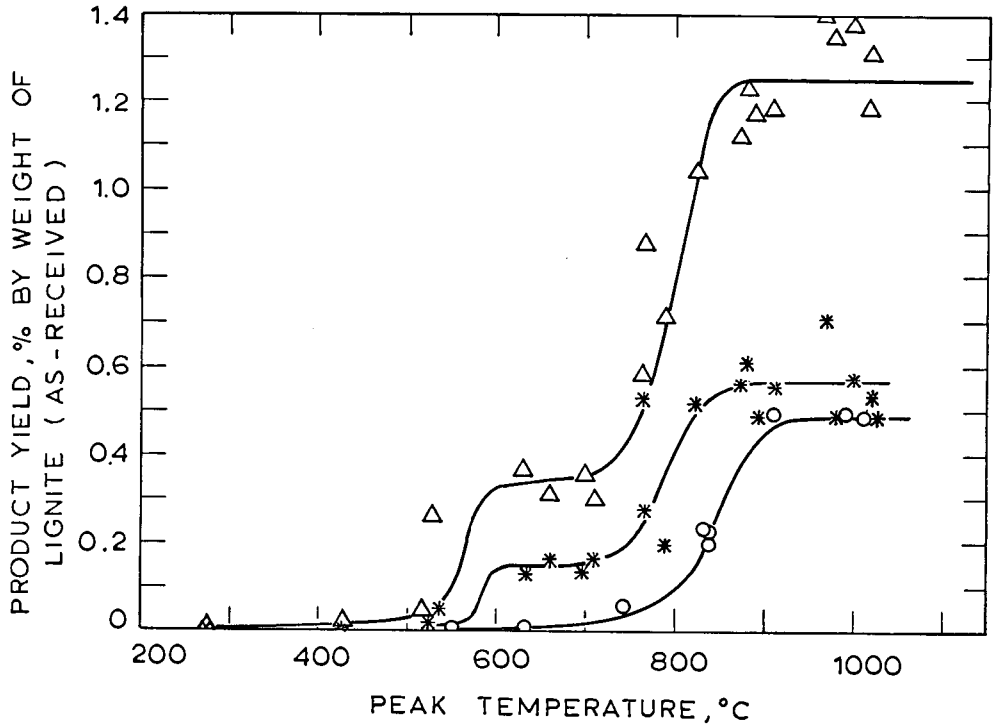

Figure 4. Yields of Methane, Ethylene and Hydrogen from Lignite Pyrolysis to Different Peak Temperatures [(Δ) CH_4; (*) C_2H_4; (o) H_2. Pressure = 1 atm (helium). Heating rate = 1000°C/s].

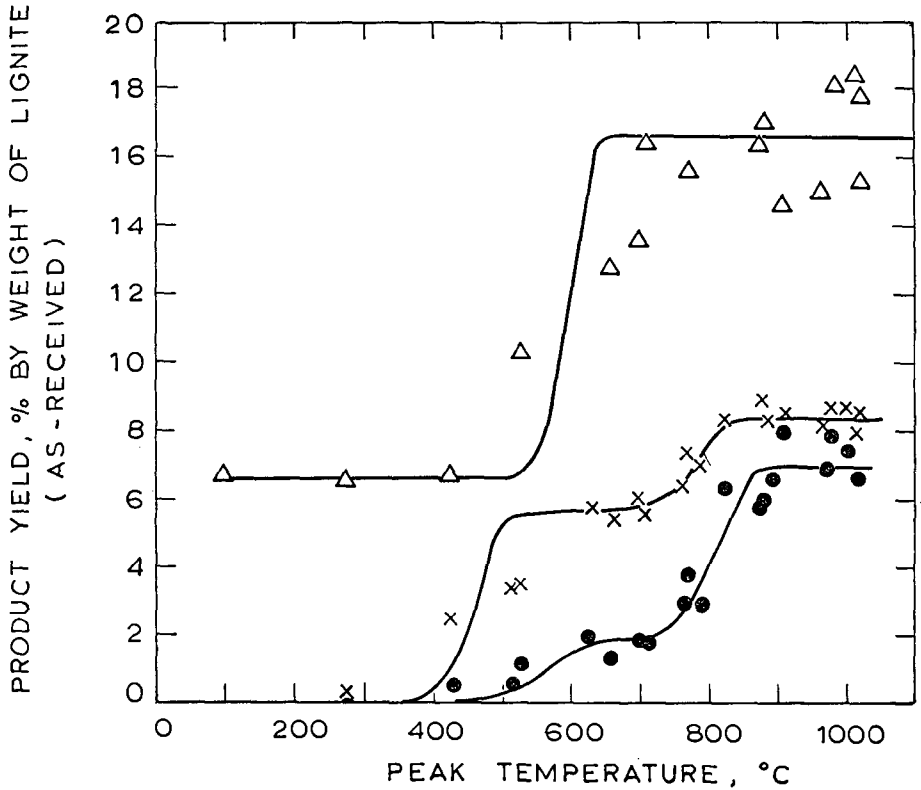

Figure 5. Yields of Water, Carbon Monoxide, and Carbon Dioxide from Lignite Pyrolysis to Different Peak Temperatures [(Δ) H_2O; (x) CO_2; (●) CO. Pressure = 1 atm (helium). Heating rate = 1000°C/s].

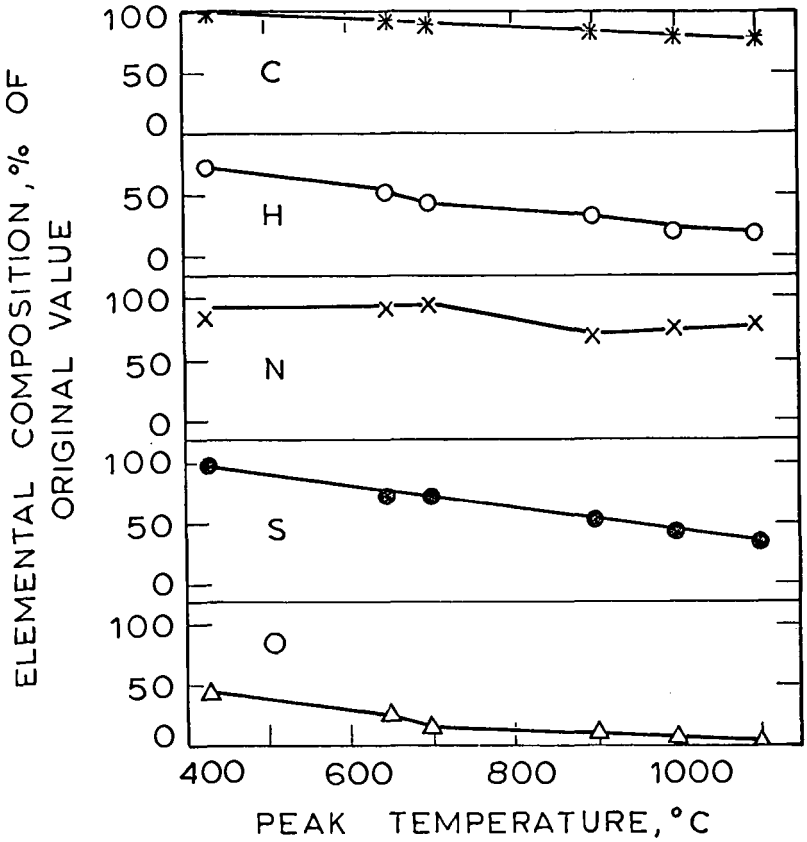

Figure 6. Elemental Compositions of Chars from Lignite Pyrolysis to Different Peak Temperatures [(*) C; (o) H; (x) N; (●) S; (Δ) O. Pressure = 1 atm (helium). Heating rate = 1000°C/s].

Table 2. Carbon, Oxygen, Hydrogen and Total Mass Balances

Product	Yield, weight % of Lignite (as-received)+, in Four Runs to Different Peak Temperatures															
	430°C				710°C				910°C				1000°C			
	Total	C	H	O	Total	C	H	O	Total	C	H	O	Total	C	H	O
CO_2	2.5	0.68	-	1.8	5.5	1.5	-	4.0	8.6	2.3	-	6.3	8.7	2.4	-	6.3
CO	0.46	0.20	-	0.26	1.8	0.77	-	1.0	8.0	3.4	-	4.6	7.5	3.2	-	4.3
HC*	0.02	0.02	0.0	-	0.95	0.79	0.17	-	2.6	2.1	0.49	-	3.0	2.4	0.58	-
Tar	1.5	1.3	0.15	-	2.3	2.1	0.23	-	4.9	4.4	0.49	-	4.7	4.3	0.47	-
H_2O	6.6	-	0.73	5.9	16	-	1.8	14	15	-	1.7	13	19	-	2.1	17
H_2	0.0	-	0.0	-	0.01	-	0.01	-	0.50	-	0.50	-	0.50	-	0.50	-
Char	89.0	64.0	3.9	10.0	73.0	53.6	2.3	2.9	60.9	47.5	1.8	2.0	55.8	44.2	1.0	1.1
Total	100	66.2	4.78	18.0	99.9	58.8	4.51	21.9	101	59.7	4.98	25.9	99.2	56.5	4.65	28.7
Closure	100%	112%	90%	77%	100%	99%	85%	93%	101%	101%	94%	110%	99%	95%	88%	122%

*Hydrocarbons other than tar.

+Lignite (as-received) is 59.3%C, 5.29%H, and 23.5%O, including H and O in lignite moisture.

difference, uncertainties inherent in the other measurements are absorbed in the oxygen values.

Product heating value contents -- i.e., mass yield x net (lower) heating value on a mass basis -- shown in Fig. 7 were estimated from the product yields in Table 2 and some additional tar and gas measurements. Heating values of the lignite and char were calculated from the elemental analyses (Table 1 and Fig. 6) using the correlation of Mott and Spooner (9) here adjusted to a net-heating value, as-received basis. The net heating value of the tar and that of hydrocarbons other than methane, ethylene and tar were assumed to be 16,000 and 19,700 Btu (37.2 and 45.8 KJ/g) respectively. The heating values of the methane, ethylene, hydrogen and carbon monoxide were, of course, known.

The heating value contents of the gas and tar follow the two-step behavior associated with the appearance of many of the individual components. At the higher temperatures, the gas accounts for a maximum of almost 15 % of the heating value content initially in the lignite, and the tar for about 8 %. At a temperature of about 1000°C, the char retains almost 70 % of the heating value on the same basis. The volumetric net heating value of the gas produced at peak temperatures above about 900°C is about 380 Btu/std. cu. ft. (14.2 MJ/m^3) on a dry basis.

The total heating value content of all products appears first to increase and then to decrease as the peak temperature increases. Pyrolysis appears to be endothermic over a range of lower to intermediate temperatures where the total heating value content of all the products is greater than that of the starting material. At higher temperatures, however, the total becomes less than the initial value and therefore pyrolysis to those temperatures may be thermally neutral or exothermic. The approximations used in this analysis preclude quantitative assessment of heats of pyrolysis.

Effect of Temperature-Time History Data points inside squares in Fig. 3 were obtained with the base conditions given above but modified as follows. The lignite was first heated to an intermediate temperature and then cooled to room temperature as before. The resulting char was then heated to a higher temperature and again cooled. The figure shows cumulative product yields for both cycles. The intermediate temperatures for the points at 855°C and 1070°C are 480°C and 670°C, respectively. The yields of all products in both cases are not significantly different from those obtained when the lignite is heated directly to the final peak temperature. This observation is consistent with the previous conclusion from weight loss data (3,4) that the pyrolysis reactions occurring at higher temperatures are largely independent of those occurring at lower temperatures. Such behavior is indicative of multiple parallel independent reactions as opposed to competitive reactions.

The encircled data points in Fig. 3 were obtained at heating rates of 7,100 to 10,000°C/s which is approximately ten-times higher than that of the base data. The points in triangles represent data taken at 270 to 470°C/s. No clear effect of heating rate is observed over the range here used. It is shown below that this behavior is expected for independent parallel, rather than competitive reactions.

Effect of Pressure Some runs were conducted under vacuum conditions (0.05 mm Hg; 7 Pa). Up to a temperature of 800°C, the total yield of volatiles and their composition are indistinguishable from those produced under 1 atm (101.3 kPa) of helium at roughly the same heating rates. Above 800°C, however, observable differences are noted in both total yield and product composition. The differences occurring at a peak temperature of 1000°C can be seen in Table 3. The temperature dependence of the pressure effect on the yields of some key components is shown in Fig. 8. Collection of all the tar formed under vacuum is difficult. Whereas at atmospheric pressures most of the tar stays suspended as an aerosol until it is purged through the filter, tar produced under vacuum deposits uniformly across all

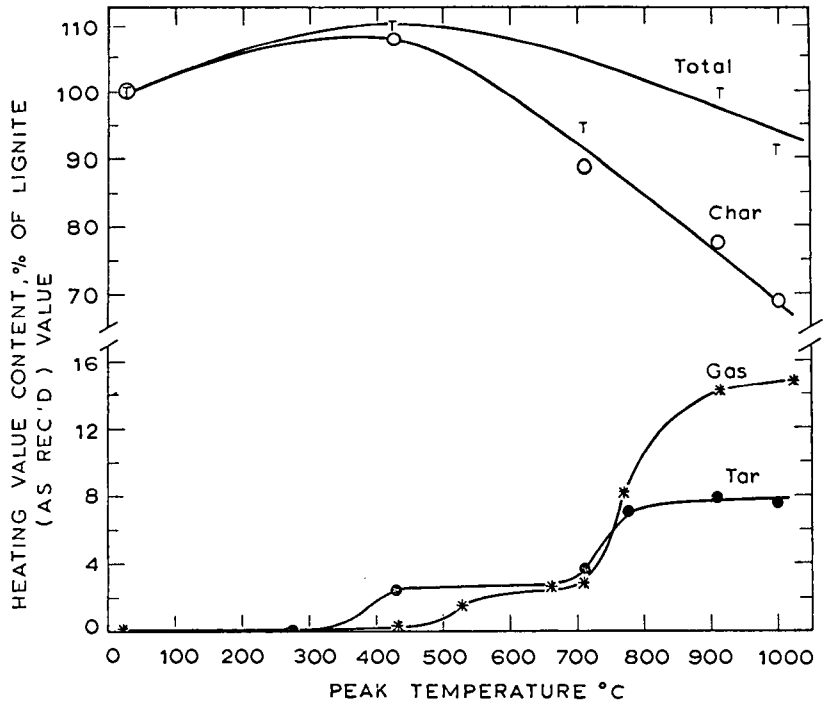

Figure 7. Distribution of Heating Value Content of Products from Lignite Pyrolysis to Different Peak Temperatures [(T) total, all products including char; (o) char; (*) gas; (•) tar. Pressure = 1 atm (helium). Heating rate = 1000°C/s. Basis: 100% on ordinate corresponds to 9,900 Btu/lb (23 KJ/g) lignite (as-received), the initial net (lower) heating value].

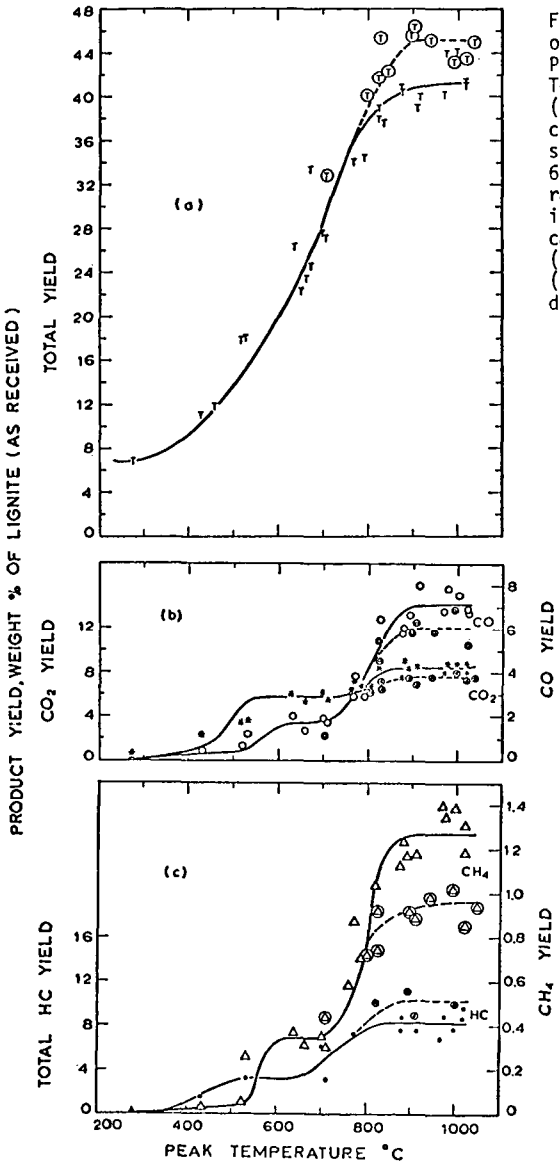

Figure 8. Effect of Pressure on Product Yields from Lignite Pyrolyzed to Different Peak Temperatures [Pressure: (single points and solid curves) 1 atm; (points inside 0 and dashed curves) 6.6 x 10^{-5} atm. Heating rate = 1000°C/s. (T) total, i.e., tar, all other hydrocarbons, H_2O, CO_2 and CO; (o) CO; (*) CO_2; (Δ) CH_4; (●) total hydrocarbons including tar].

Table 3. Effect of Pressure on Lignite Pyrolysis Product Yields (Peak temperature, 1000°C; heating rate, 1000°C/s)

Product	Yield, wt% of lignite (as received)	
	1 atm. He	vacuum
CO	7.1	6.1
CO_2	8.4	7.6
CH_4	1.3	0.95
C_2H_4	0.56	0.45
HC*	0.95	2.0
Tar	5.4	6.9
H_2O	16.5	18.1
H_2	0.50	N.M.**
Total Products	40.7	42.1
Measured Wt. Loss	41.3	44.7

*All hydrocarbons other than Tar, CH_4, and C_2H_4.
**Not measured

reactor surfaces upon initiation of the purge. Recovery of the thin tar film by the methylene chloride washing procudure is somewhat inefficient. Thus the total mass balance is poorer at vacuum than at 1 atm. A carbon balance conducted as described for Table 2 shows a carbon dificit of about 3 % for the vacuum data in Table 3. Therefore the actual vacuum tar yield at 1000°C may be about 9 % of the lignite weight.

The main conclusion from Table 3 and Fig. 8 is that vacuum pyrolysis of lignite produces higher yields of heavy hydrocarbon products and lower yields of light gases than are obtained at 1 atm. Since also the total weight loss is higher under vacuum, it appears that secondary cracking and char forming reactions play a role in determining product yields. In view of the thin layer of coal employed, the main contribution of the secondary reactions in this experiment presumably occurs within the particles. A similar but quantitatively more significant effect of secondary reactions on total weight loss from a bituminous coal was observed by Anthony et al.(3,4). Other workers(10,11) also have observed increased yields of low-volatile species in vacuum pyrolysis of coal.

MODEL

The modelling of coal pyrolysis as a set of independent parallel reactions having a statistical distribution of activation energies has been shown to provide valuable insight into the overall or global kinetics of the process(3). With the products in the present study dominated by a few individual species and classes of species, e.g. tar, there is interest in determining whether pyrolysis can be effectively modelled as only a few reactions representing the production of these key products.

As a first test of this approach, the appearance of product i is modelled as a reaction first-order in the amount of i yet to be produced. Thus for the reaction

$$\text{Coal} \rightarrow \text{Product}_i \qquad (1)$$

the assumed first-order rate is

$$dV_i/dt = k_i(V_i^* - V_i) \qquad (2)$$

and the rate constant is assumed to be

$$k_i = k_{io} \exp(-E_i/RT) \qquad (3)$$

where k_{io} is the pre-exponential factor, E_i is the activation energy of reaction i, V_i is the amount of product i produced up to time t, V_i^* is the amount of product i which could potentially be produced, (i.e., at $t = \infty$), T is the absolute temperature, and R is the gas constant. Assuming that temperature increases linearly with time, as it does in our experiments, with the constant rate $dT/dt = m$, solution of the above equations gives

$$\int_0^{V_i} dV_i/(V_i^* - V_i) = \int_0^T (k_{io}/m) \exp(-E_i/RT)dT \quad (4)$$

Since $E_i/RT >> 1$ is a good approximation for coal decomposition reactions, the solution becomes

$$(V_i^* - V_i)/V_i^* = \exp[-(k_{io}RT^2/mE_i)\exp(-E_i/RT)] \quad (5)$$

This equation is plotted in Fig. 9 for activation energies typical of organic decomposition reactions (see Table 4) and a typical pre-exponential factor of $k_{io} = 1.67 \times 10^{13} s^{-1}$. The inadequacy of the single-reaction model in fitting the data on total yield of volatiles is evident from this figure; nevertheless, this approach has been taken by many workers for correlating pyrolysis data.

It can be seen from the wide range of materials listed in Table 4 that organic decomposition reactions encompass a wide range of activation energies and pre-exponentials. It is not surprising that coal, the chemical structure of which is far more complex than that of the materials in Table 4, decomposes thermally to produce numerous products and that these products exhibit different activation energies. When a single first-order reaction is used to model coal pyrolysis, the activation energy and pre-exponential factor are forced to be very low in order to fit the overall temperature dependence that actually results from the occurrence of different reactions in different temperature intervals. The results are sometimes interpreted as reflecting transport limitations because the parameters are too low for organic decompositions. This point is further discussed elsewhere(5).

Considerably more success is attained when the first-order model is applied to the appearance of single products. As is implied in Figs. 3 to 5, many individual species are not adequately described by one first-order process. Rather than utilizing a large number of parallel reactions with a distribution of activation energies for individual species(18), a simplifying assumption is made that one, two or three parallel reactions, depending on the observed behavior, describes the formation of certain key products. The mechanistic implication is that a given species may arise from more than one type of reactant, or from more than one reaction pathway.

The first-order model was used with the measured time-temperature history of each experimental run to construct best fit curves for the yield data. The resulting kinetic parameters are summarized in Table 5. The curves shown in Figs. 3,4, and 5 were calculated using these parameters and the model, for a standardized experiment in which coal is heated at 1000°C/s to the peak temperature, and then cooled at 200°C/s back to room temperature. The curves fit the data well for most species, and modelling with only one or two reactions appears sufficient in all cases except the carbon oxides which require a third reaction for data above about 1000°C (not shown here). Figure 3 shows how the various individual reactions cooperate to give a smooth total weight loss curve. Again, this figure emphasizes that a large fraction of the total weight loss is due to the oxygenated species.

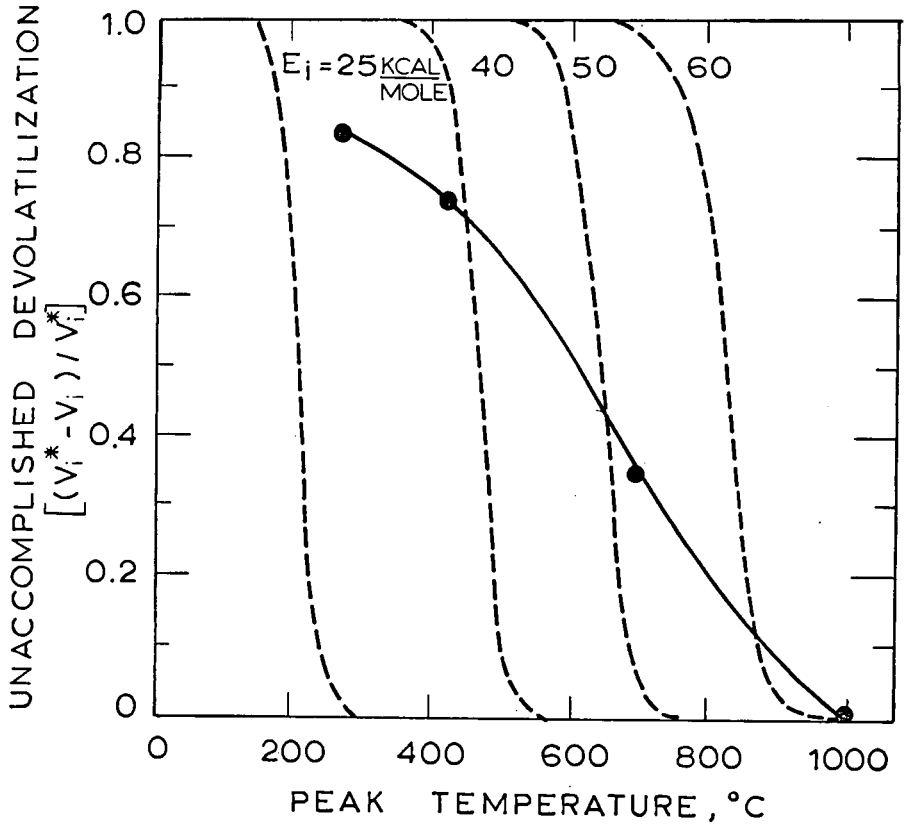

Figure 9. Comparison of Data on Overall Conversion of Lignite to Volatiles with Predictions from Single-Step First-Order Pyrolysis Model [(•) data; (dashed curves) predictions from model].

Table 4. Kinetic Parameters for Pyrolysis of Various Organic Materials

Material Pyrolyzed	Product[a]	Experimental Temp., °C	Activation Energy, kcal/mole	Pre-Exponential Factor, s^{-1}	Ref.
Ferulic Acid ($C_{10}H_{10}O_4$)	CO_2	150-250	27.7	6.0×10^{9}	12, 13
Perylene Tetracarboxylic Acid Anhydride ($C_{24}H_8O_6$)	CO_2	400-600	71.5	5.2×10^{17}	12, 13
	CO	400-600	64.9	5.0×10^{16}	12, 13
Protocatechuic Acid ($C_7H_6O_4$)	$(H_2O)_1$	50-300	18.8	2.7×10^{8}	12, 13
	$(H_2O)_2$	50-300	42.4	2.3×10^{5}	12, 13
	CO_2	50-300	40.4	1.6×10^{15}	12, 13
Naphthalene Tetracarboxylic Acid ($C_{14}H_8O_8$)	H_2O	100-250	33.5	1.2×10^{13}	12, 13
Mellitic Acid ($C_{12}H_6O_{12}$)	H_2O	230[b]	16.6	2.3×10^{5}	13
Tartaric Acid ($C_4H_6O_6$)	H_2O	195[b]	42.9	6.7×10^{17}	13
Polystyrene $(C_8H_8)_n$	overall	394[b]	77	8.3×10^{22}	13
	overall	335-355[b]	58	9.0×10^{15}	14
Teflon $(C_2F_4)_n$	overall	575[b]	67-69	4.3×10^{14}	13
Polyethylene $(C_2H_4)_n$ "Phase 1"	overall	385-405	48	5.2×10^{11}	14
"Phase 2"	overall	385-405	71	8.7×10^{18}	14
Hydrogenated Polystyrene $(C_8H_{14})_n$	overall	335-350	52	1.4×10^{14}	15
Polymeta-methylstyrene $(C_9H_{10})_n$	overall	333-353	50	7.2×10^{16}	15
Polyalpha-methylstyrene $(C_9H_{10})_n$	overall	273-288	58	8.3×10^{18}	15
Polymethyl-methacrylate $(C_5H_8O_2)_n$					
Avg. Molecular Wt. 150,000	overall	240-270	33	3.6×10^{9}	15
Avg. Molecular Wt. 5,100,000	overall	310-325	55	1.8×10^{16}	15
Polymethylacrylate $(C_4H_6O_2)_n$	overall	285-300	37	1.4×10^{10}	15
Cellulose $(C_6H_{10}O_5)_n$	overall	250-1000	33.4	6.8×10^{9}	16
		250-350	35	3.3×10^{11}	13, 17

a. Denotes species whose evolution is described by the parameters given. Two different stages of water evolution are denoted by $(H_2O)_1$ and $(H_2O)_2$. Overall refers to all products combined.

b. Temperature of maximum pyrolysis rate.

Table 5. Kinetic Parameters for Lignite Pyrolysis

Product	Stage	E_i, kcal/mole	log (k_{io}/s^{-1})	V_i^*, Wt.% of lignite (as-received)
CO_2	1	36.2	11.33	5.70
	2	64.3	13.71	2.70
	3	42.0	6.74	1.09
CO	1	44.4	12.26	1.77
	2	59.5	12.42	5.35
	3	58.4	9.77	2.26
CH_4	1	51.6	14.21	0.34
	2	69.4	14.67	0.92
C_2H_4	1	74.8	20.25	0.15
	2	60.4	12.85	0.41
HC[a]		70.1	16.23	0.95
Tar	1	37.4	11.88	2.45
	2	75.3	17.30	2.93
H_2O		51.4	13.90	16.5
H_2		88.8	18.20	0.50
Total				44.0

a. Hydrocarbons other than CH_4, C_2H_4 and Tar

Examination of Fig. 3 also reveals that there are apparently five principal phases of devolatilization. The first occurs at very low temperatures (~100°C) and is associated with moisture evolution. The second phase at 1000°C/s heating rate begins at about 450°C and is associated with a large initial evolution of carbon dioxide, probably from low-activation energy decarboxylations. The loss of carboxyl groups as carbon dioxide at relatively low temperatures has been reported for lignites(10). A small amount of tar is also evolved at this stage. This material may contain not only real tar (e.g., asphaltenes and heavy oils) but also small particles of lignite broken off the parent particles by the escaping gases as mentioned above. The third phase involves evolution of water chemically formed in the range 500-700°C where the only other significant product is carbon dioxide. It can be seen from Fig. 6 that carbon, nitrogen and sulfur during this phase remain largely in the char while the oxygen and hydrogen contents of the char sharply decrease. The fourth phase involves a final rapid evolution of carbon containing species. Carbon oxides, tar, hydrogen, and hydrocarbon gases are all rapidly evolved in the temperature range 700-900°C, where little water is produced. The fifth phase is the previously discussed high temperature formation of carbon oxides. To be compared with the foregoing, Chukhanov(19) suggests that coal pyrolysis involves three stages: evolution of carbon oxides and water (450-550°C); formation of tar and hydrocarbon gases; and residue degasification.

In order to compare the present kinetic parameters with those obtained before using a distributed activation energy model(1,3-5), the frequency distribution of the present activation energies is derived from Table 5 as follows. Data points in Fig. 10 represent the cumulative ultimate yields of all volatile components having activation energies less than or equal to those of the indicated points. Each point is labelled with the component whose ultimate yield is added to those

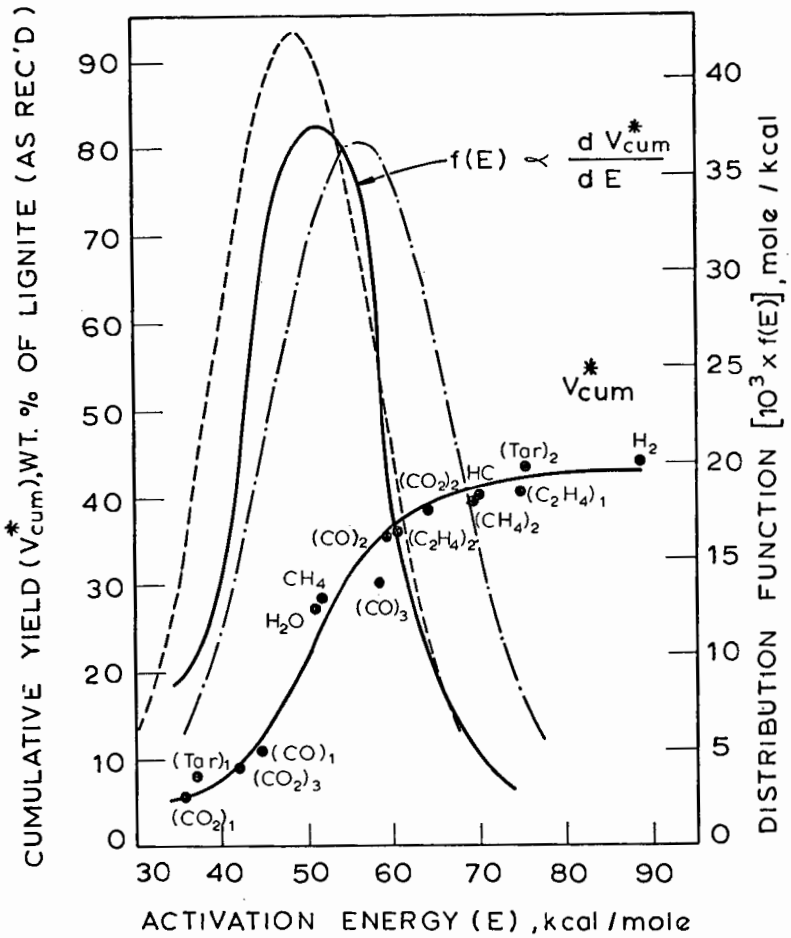

Figure 10. Distribution of Activation Energies of Pyrolysis Reactions [(●) cumulative yields, from present base data, of components indicated to left of and including a given point; (solid curves) present results based on volatiles yields; (broken curves) previous results [1,5] based on weight loss data and two different sets of kinetic parameters].

of all other components shown on points to the left to give the indicated cumulative yield; e.g., the vertical distance between two adjacent points represents the ultimate yield of the component specified on the higher point. The slope of the smooth curve drawn through the data gives the frequency distribution curve $dV^*_{cum}/V^*_{tot}dE$, which is here normalized so that the area under a segment of the curve between two values of activation energy is the percentage of the total ultimate volatile yield that is associated with activation energies in the specified interval.

Figure 10 also presents two distributions (broken curves) obtained previously(1,5) for the same lignite as was used here, but from a kinetic analysis of weight loss data using a statistically large number of reactions having a Gaussian distribution of activation energies and all having the same pre-exponential factor. The left-hand curve was obtained when the pre-exponential factor (k_o=1.07x$10^{10}s^{-1}$) was evaluated as one of the adjustible parameters, while the right-hand curve was obtained using a preferred fixed value of k_o(1.67x$10^{13}s^{-1}$). The mean activation energies (E_o) and standard deviations (σ) of the previous distributions are, in kcal/mole, (left) E_o=48.7 and σ=9.38 and (right) E_o=56.3 and σ=10.9. Statistical analysis shows that the present data are not significantly different from a Gaussian distribution with E_o and σ being 53.3 and 11.5 kcal/mole, respectively. The similarity of the present distribution derived from product compositions to the previous results based on weight loss is especially encouraging since k_o, which does influence E_o, was here allowed to assume a different value for each reaction whereas previously a single k_o was used for all reactions.

DISCUSSION

Since coal is always "hydrogen-starved" in the sense that its empirical formula is usually $CH_{0.6}$ to CH (the present lignite is roughly $CH_{0.9}$) while the desired products are in the range CH to CH_4, it is desirable to use the coal hydrogen as efficiently as possible. The oxygen in the coal removes most of the hydrogen at temperatures below those at which the principal hydrocarbon forming reactions can occur; thus, by the time the coal is hot enough for the latter reactions to occur, there is too little hydrogen left to produce stable, volatile fragments. The addition of hydrogen from outside the particle, e.g., as in the case of hydrogasification, enhances the yield of volatiles perhaps by stabilizing some reactive sites or species that would otherwise form char(4,5,20-23). This hypothesis will be tested with future experiments in a hydrogen atmosphere.

If the pyrolysis reactions that form water and hydrocarbons are in competition for hydrogen, then the hydrocarbon yield could perhaps be increased by subjecting the coal to a favorable time-temperature history. For example, in the present results tar forming reactions have a higher activation energy than the water forming reactions (75.3 kcal/mole compared to 51.4 kcal/mole) and hence are favored by going to higher temperatures. According to the present model, very high rates of heating would be required to attain these higher temperatures without the water forming reactions first reaching completion. At 1000°C/s, the water forming reactions are about 90 % complete before the onset (defined as 1 % completion) of the tar forming reactions. This analysis neglects the low temperature tar forming reactions and also assumes that the water and tar forming reactions are independent. At 6090°C/s, the water forming reaction are predicted to be 75 % complete when the onset of tar formation occurs (at 700°C), and at 2.8x10^5°C/s, the water reactions are only 35 % complete at the onset of tar formation (at 800°C). Total volatile yields significantly larger than those of the present study were in fact observed(7,8) from Montana lignite heated at about 2x10^5°C/s to about 1800°C.

It is interesting to compare the observed product distributions with those that would be obtained if all the volatiles generated in a run were in mutual equilibrium in the presence of char at the final temperature of the particles. For approximation purposes the char is assumed to be graphite and the mole fraction of the ambient helium adjacent to and within the particles is assumed to be negligible. Equilibrium relations for the reactions

$$CO + H_2O = CO_2 + H_2 \quad (6)$$

$$C + H_2O = CO + H_2 \quad (7)$$

$$C + 2H_2 = CH_4 \quad (8)$$

$$CH_4 + H_2O = CO + 3H_2 \quad (9)$$

in the presence of excess solid carbon are shown as curves in Fig. 11 where the base data are given as points. Two cases are considered, one including water from the lignite moisture in the volatiles (points) and the other including only the chemically formed water (not shown). The latter case covers the possibility that moisture is lost early enough so as to be absent from the reacting mixture. The complete or partial loss of others products could also be considered but this was not done since moisture loss, which appears to offer the largest potential for an effect, is found to be of little significance in this rough analysis.

Figure 11 shows that the data tend toward less disagreement with the equilibrium values as temperature increases. When the total pressure of volatiles is assumed to be 1 atm, which is the experimental pressure under which the data were taken, all the reactions are far from equilibrium with the exception of Reaction 6 at the higher temperatures, where a rather close approach to equilibrium cannot be excluded within the large uncertainty of this calculation. Reaction 6 is the only one of the four that is independent of pressure. The equilibrium values for the other reactions also agree roughly with the data if the assumed total pressure of the volatiles is increased substantially, the values for Reactions 7,8, and 9 depending on pressure to the powers -1, +1, and -2, respectively.

Volatiles pressures much larger than 1 atm within the pores of the particles are not inconsistent with calculated pressure drops associated with volatiles explusion under the present conditions of rapid pyrolysis. The agreement in Fig. 11 between the equilibrium values and the data for an assumed pressure of 1000 atm is intriguing. We do not know to what extent such a high pressure properly reflects conditions developed within rapidly pyrolyzing lignite, but we note that internal pressures of this order of magnitude (a) would be calculated if it is assumed that the formation of volatiles within the pores largely precedes the escape therefrom, and (b) would appear to be required to fracture the particles based on the strength of the material. Lignites rapidly heated are known to exhibit fracturing or "sparking", a phenomenon that could account for the particulate material here found in the tar as noted above.

Although the foregoing equilibrium analysis is far from definitive, it is probably safe to conclude that the final mixture of volatiles is closer to equilibrium than are the primary volatiles and, therefore, that mass transport and secondary reactions within the particles do play some role in determining product distributions. Thus, at temperatures above about 800°C, the enhanced mass transport condition provided by vacuum pyrolysis leads to somewhat higher yields of hydrocarbon liquids and tars and correspondingly lower yields of light hydrocarbon and carbon oxide gases. The behavior indicates that more volatiles cracking within particles occurs at 1 atm than under vacuum, but the difference affects no more than about 5 % of the total lignite material. The fact that this effect is small supports the picture that the pressure inside lignite particles during rapid pyrolysis is indeed high and therefore not strongly dependent on external pressure in

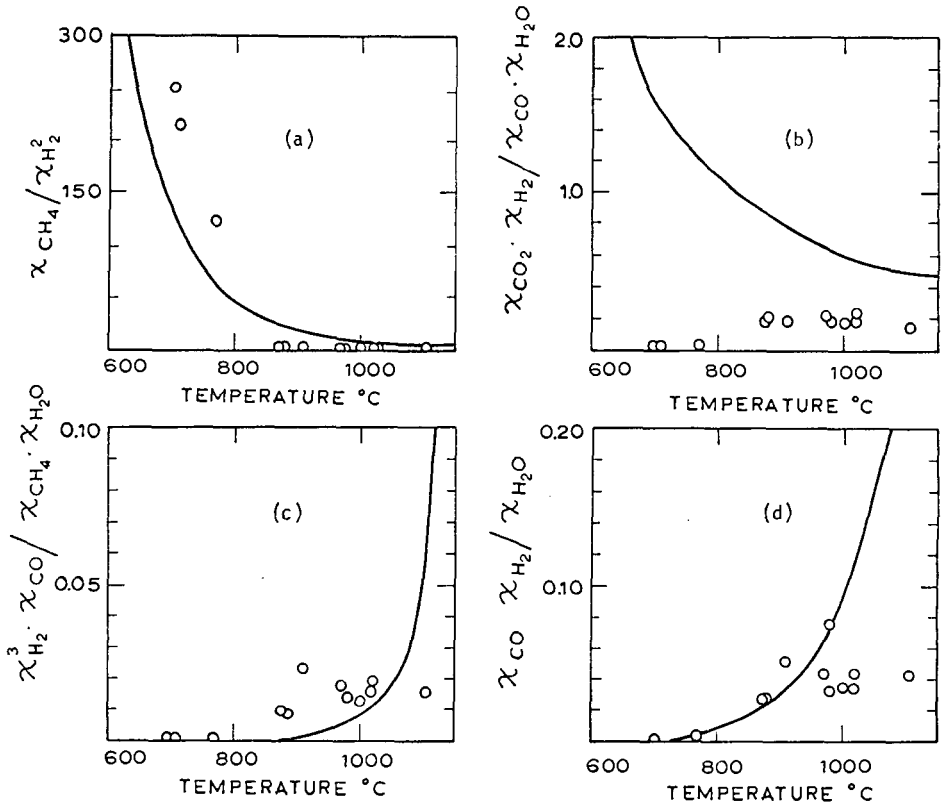

Figure 11. Comparison of Gas Composition Data for Different Peak Temperatures with Calculated Equilibrium Values under Simplified Conditions [χ_i = mole fraction of i. (o) base data; (curves) equilibrium values multiplied by 10^3 in (a), 1 in (b), 10^{-6} in (c) and 10^{-3} in (d), all these factors being equivalent to the assumption that the total partial pressure of volatiles is 10^3 atm].

the range 0 to 1 atm. Accordingly, the absolute amount of volatiles cracking within the pores may be much larger than the change observed in going from 1 atm to vacuum conditions.

The suggested role of mass transport and secondary reactions points up the empirical nature of pyrolysis models, such as the one employed here, that do not explicitly account for these effects. The kinetic parameters obtained by application of the present multiple parallel reaction model to species originating in some combination of primary and secondary reactions are clearly overall properties. Derivation from the present data of fundamental properties of the primary pyrolysis reactions must await a better understanding of mass transfer and secondary reactions in the particles. Nevertheless, the demonstrated success of the present model in correlating the data means that the multiple parallel reaction picture together with the identification from the data of key "reactions" (e.g., stages in the evolution of a given product species) is an effective representation of primary reactions as modified by the effects of mass transport and secondary reactions.

ACKNOWLEDGEMENT

We are grateful to the National Science Foundation, Research Applied to National Needs (RANN), for funding under Contract AER 75-13673; to Kevin E. Bennet, Richard N. Caron, Karen J. Hladik and Scott Free for valuable laboratory work; to William DuBroff of Inland Steel Research Laboratories for petrographic analysis for the lignite; and to the Institute of Gas Technology and Knife River Coal Company for lignite samples. One of us (E.S.) gratefully acknowledges personal support through the N.S.F. Energy Trainseeship program.

NOMENCLATURE

E = activation energy, kcal/mole

E_i = activation energy of reaction forming product i, kcal/mole

E_0 = mean of activation energy distribution, kcal/mole

$f(E)$ = activation energy distribution function, mole/kcal

k_i = first-order rate constant of reaction forming product i, s^{-1}

k_{io} = pre-exponential factor in k_i, s^{-1}

k_o = pre-exponential factor when all k_{io} are assumed equal, s^{-1}

m = constant heating rate, °C/s

R = gas constant, kcal/mole K

t = time, s

T = absolute temperature, K

V_i = amount of product i generated up to time t, fraction of the original coal weight

V^*_i = value of V_i at $t = \infty$ (ultimate yield), approximated by measurements at long reaction times, fraction of the original coal weight

V^*_{cum} = sum of V^*_i for all i with $E_i \leq E$, fraction of the original coal weight

V^*_{tot} = sum of all V^*_i, fraction of the original coal weight

σ = standard deviation of activation energy distribution, kcal/mole

x_i = mole fraction of component i

REFERENCES

1. Anthony, D.B., "Rapid Devolatilization and Hydrogasification of Pulverized Coal," Sc. D. thesis, Massachusetts Institute of Technology, Cambridge, Mass., 1974.

2. Anthony, D.B., J.B. Howard, H.P. Meissner, and H.C. Hottel, "Apparatus for Determining High Pressure Coal-Hydrogen Reaction Kinetics under Rapid Heating Conditions," Rev. Sci. Instrum. 45, 992 (1974).

3. Anthony, D.B., J.B. Howard, H.C. Hottel, and H.P. Meissner, "Rapid Devolatilization of Pulverized Coal," Fifteenth Symposium (International) on Combustion, p. 1303, The Combustion Institute, Pittsburgh, Pa. (1975).

4. Anthony, D.B., J.B. Howard, H.C. Hottel, and H.P. Meissner, "Rapid Devolatilization and Hydrogasification of Bituminous Coal," Fuel 55, 121 (1976).

5. Anthony, D.B. and J.B. Howard, "Coal Devolatilization and Hydrogasification," A.I. Ch.E. J. 22, 625 (1976).

6. Solomon, P.R., personal Communication (1976).

7. Kobayashi, H., "Devolatilization of Pulverized Coal at High Temperatures," Sc.D. thesis, Department of Mechanical Engineering, Massachusetts Institute of Technology, Cambridge, Mass., 1976.

8. Kobayashi, H., J.B. Howard, and A.F. Sarofim, "Coal Devolatilization at High Temperatures," Sixteenth Symposium (International) on Combustion, The Combustion Institute, Pittsburgh, Pa. (in press).

9. Mott, R.A., and C.E. Spooner, "The Calorific Value of Carbon in Coal: The Dulong Relationship," Fuel 19, 226, 242 (1940).

10. Howard, H.C., "Pyrolytic Reactions of Coal," in Chemistry of Coal Utilization, pp. 340-394, Supplementary Volume, H.H. Lowry, ed., Wiley, New York (1963).

11. Loison, R., and F. Chauvin, "Pyrolyse Rapide du Charbon," Chem. Ind. (Paris) 91, 269 (1964).

12. Jüntgen, H. and K.H. Van Heek, "Gas Release from Coal as a Function of the Rate of Heating," Fuel 47, 103 (1968).

13. Jüntgen, H. and K.H. Van Heek, "Reaktionsablaufe unter nichtisothermen Bedingungen," in Fortschritte der chemischen Forschung, vol. 13, pp. 601-699, Springer-Verlag, Berlin (1970).

14. Madorsky, S.L., "Rates of Thermal Degradation of Polystyrene and Polyethylene in a Vacuum," J. Polymer Science IX (2), 133 (1952).

15. Madorsky, S.L., "Rates and Activation Energies of Thermal Degradation of Styrene and Acrylate Polymers in a Vacuum, J. Polymer Science XI (5), 491 (1953).

16. Lewellen, P.C., W.A. Peters, and J.B. Howard, "Cellulose Pyrolysis Kinetics and Char Formation Mechanism" Sixteenth Symposium (International) on Combustion, The Combustion Institute, Pittsburgh, Pa. (in press).

17. Van Krevelen, D.W., C. Van Heerden, and F.J. Huntjens, "Physiochemical Aspects of the Pyrolysis of Coal and Related Organic Compounds," Fuel 30, 253 (1951). [Numerical results modified by Jüntgen and Van Heek (13)].

18. Hanbaba, P., H. Juntgen, and W. Peters, "Nicht-isotherme Reaktionskinetik der Kohlenpyrolyse, Teil II: Erweiterung der Theorie der Gasabspaltung und experimentelle Bestätigung an Steinkohlen," Brennstoff-Chem. 49, 368 (1968).

19. Chukhanov, Z.F., Izvest. Akad Nauk S.S.S.R., Otdel Tekh. Nauk, No. 8, pp. 7-22 (1954); Chem Abs. 49, 5808 (1955).

20. Moseley, F., and D. Paterson, "Rapid High-Temperature Hydrogenation of Coal Chars, Part 1," J. Inst. Fuel 38, 13 (1965).

21. Zahradnik, R.L. and R.A. Glenn, "Direct Methanation of Coal," Fuel 50, 77 (1971).

22. Johnson, J.L., "Kinetics of Bituminous Coal Char Gasification with Gases Containing Steam and Hydrogen," in Coal Gasification, p. 145, Advances in Chemistry Series, No. 131, Am. Chem. Soc., Washington, D.C., (1974).

23. Johnson, J.L., "Gasification of Montana Lignite in Hydrogen and in Helium during Initial Reaction Stages," Am. Chem. Soc., Div. of Fuel Chem. Preprints 20, No. 3, 61 (1975).